Atmos. Chem. Phys. Discuss., 15, 14923–14960, 2015
www.atmos-chem-phys-discuss.net/15/14923/2015/
doi:10.5194/acpd-15-14923-2015

Atmospheric Chemistry and Physics Discussions

A comparison of secondary organic aerosol (SOA) yields and composition from ozonolysis of monoterpenes at varying concentrations of NO_2

D. C. Draper[1,*], D. K. Farmer[2], Y. Desyaterik[3], and J. L. Fry[1]

[1]Department of Chemistry, Reed College, Portland, OR, USA
[2]Department of Chemistry, Colorado State University, Fort Collins, CO, USA
[3]Department of Atmospheric Science, Colorado State University, Fort Collins, CO, USA
[*]now at: Department of Chemistry, University of California Irvine, Irvine, CA, USA

Received: 25 April 2015 – Accepted: 6 May 2015 – Published: 28 May 2015

Correspondence to: J. L. Fry (fry@reed.edu)

Published by Copernicus Publications on behalf of the European Geosciences Union.

Abstract

The effect of NO_2 on secondary organic aerosol (SOA) formation from ozonolysis of α-pinene, β-pinene, Δ^3-carene, and limonene was investigated using a dark flow-through reaction chamber. SOA mass yields were calculated for each monoterpene from ozonolysis with varying NO_2 concentrations. Kinetics modeling of the first generation gas-phase chemistry suggests that differences in observed aerosol yields for different NO_2 concentrations are consistent with NO_3 formation and subsequent competition between O_3 and NO_3 to oxidize each monoterpene. α-pinene was the only monoterpene studied that showed a systematic decrease in both aerosol number concentration and mass concentration with increasing [NO_2]. β-pinene and Δ^3-carene produced fewer particles at higher [NO_2], but both retained moderate mass yields. Limonene exhibited both higher number concentrations and greater mass concentrations at higher [NO_2]. SOA from each experiment was collected and analyzed by HPLC-ESI-MS, enabling comparisons between product distributions for each system. In general, the systems influenced by NO_3 oxidation contained more high molecular weight products (MW > 400 amu), suggesting the importance of oligomerization mechanisms in NO_3-initiated SOA formation. α-pinene, which showed anomalously low aerosol mass yields in the presence of NO_2, showed no increase in these oligomer peaks, suggesting that lack of oligomer formation is a likely cause of α-pinene's near 0 % yields with NO_3. Through direct comparisons of mixed-oxidant systems, this work suggests that NO_3 is likely to dominate nighttime oxidation pathways in most regions with both biogenic and anthropogenic influences. Therefore, accurately constraining SOA yields from NO_3 oxidation, which vary substantially with the VOC precursor, is essential in predicting nighttime aerosol production.

ACPD
15, 14923–14960, 2015

1 Introduction

Secondary organic aerosol (SOA) forms in the atmosphere from oxidized volatile organic compounds (VOCs) that are of low enough volatility to be able to partition into the condensed phase. Aerosol directly affects Earth's radiative balance and also contributes to cloud formation, both of which have important climate forcing implications (IPCC, 2013). Aerosol is responsible for regional haze, and has been shown to cause adverse cardiopulmonary health effects (Pope III et al., 1995; Davidson et al., 2005). SOA constitutes a large fraction of the total aerosol budget, but it is still poorly constrained in global chemical transport models, which underpredict ambient aerosol concentrations by one to two orders of magnitude (Heald et al., 2005, 2011). These models use laboratory-derived parameters, but uncertainty in precursors, detailed mechanisms, and mechanistic differences between chamber simulations and the real atmosphere result in the vast discrepancies between models and observations (Kroll and Seinfeld, 2008; Hallquist et al., 2009).

Nearly 90 % of the non-methane VOCs emitted globally are biogenic in origin, so it should follow that a large fraction of the uncertainty in model predictions of the SOA budget comes from uncertainty in how biogenic VOCs (BVOCs) form aerosol (Guenther et al., 1995; Middleton, 1995). Different plant species emit different types and ratios of BVOCs, so the specific distribution of BVOCs emitted to the atmosphere is dependent on unique mixtures of vegetation and thus varies a great deal regionally. Monoterpenes are one such class of BVOC that is both widely emitted and has been shown in the laboratory to efficiently produce SOA (Goldstein and Galbally, 2007; Sakulyanontvittaya et al., 2008; Griffin et al., 1999; Hallquist et al., 1999; Ng et al., 2006; Ehn et al., 2014; Hoyle et al., 2011). On average in the US, α-pinene is the most dominant monoterpene emission, but β-pinene, Δ^3-carene, and limonene (Fig. 1) are also prevalent and are emitted equally or more than α-pinene in some regions (Geron et al., 2000).

While most VOCs are biogenic, the majority of atmospheric oxidants are anthropogenically sourced, and thus human activity is highly influential on SOA production

ACPD
15, 14923–14960, 2015

(Carlton et al., 2010). At night, most VOC oxidation in the troposphere occurs by way of either photolabile nitrate radical (NO_3) or longer-lived ozone (O_3), which is photochemically produced but is not rapidly and completely consumed at sundown as is the hydroxyl radical (OH). The formation of both of these tropospheric oxidants requires NO_2, nearly 90 % of which in the US (64 % globally) is estimated to come from anthropogenic sources (Reis et al., 2009). Organonitrates have been observed in ambient nighttime aerosol during multiple field studies (Fry et al., 2013; Rollins et al., 2012; Xu et al., 2015), consistent with NO_3 oxidation, and NO_3 initiated production of aerosol organonitrates may even be competitive during the day in some regions with high BVOC emissions (Ayres et al., 2015). These observations are consistent with several laboratory studies that have found moderate to high aerosol yields from NO_3 oxidation (Griffin et al., 1999; Hallquist et al., 1999; Fry et al., 2009, 2011, 2014; Spittler et al., 2006; Moldanova and Ljungström, 2000), but this body of literature is comparatively small relative to OH and O_3 oxidation studies.

Most chamber studies of NO_3-derived SOA generate NO_3 through the thermal dissociation of N_2O_5 in order to minimize the complexity caused by introducing a second oxidant (Griffin et al., 1999; Hallquist et al., 1999; Fry et al., 2014). Fewer studies have been done using the atmospherically more relevant conditions of introducing both O_3 and NO_2 into the chamber to mimic this full range of nighttime oxidation chemistry (Perraud et al., 2012; Presto et al., 2005; Boyd et al., 2015). Perraud et al. (2012) and Presto et al. (2005) both studied the effects of a range of NO_2 concentrations on dark ozonolysis of α-pinene, and both observed that increased [NO_2] suppresses aerosol formation. To our knowledge, NO_2 effects on dark ozonolysis have not been assessed for any other monoterpenes. Ozonolysis of α-pinene has been previously observed to have high aerosol yields (Ng et al., 2006) but strikingly low (0–16 %) SOA yields with NO_3 (Hallquist et al., 1999; Fry et al., 2014; Spittler et al., 2006). The observed aerosol suppression in the $O_3 + NO_2$ system is consistent with the increased contribution of NO_3 at higher [NO_2]. However, α-pinene is the only monoterpene that has been observed to have such drastic SOA yield discrepancies between the two oxidants (Ng

ACPD
15, 14923–14960, 2015

et al., 2006; Yu et al., 1999; Hallquist et al., 1999; Fry et al., 2014), so it may not be reasonable to assume NO_2 has the same effect on other monoterpenes.

Here we focus on the four most prevalently emitted monoterpenes in the US: α-pinene, β-pinene, Δ^3-carene, and limonene. Table 1 shows rate constants for NO_3 formation from $NO_2 + O_3$ as well as each of the nighttime oxidants with the monoterpenes used in this study. It is evident that the rates of O_3 loss to NO_3 production and BVOC oxidation are comparable when [NO_2] and [BVOC] are similar. Even considering its smaller ambient concentrations, NO_3 oxidation is often much faster than O_3 oxidation, so it follows that NO_3 oxidation should provide an important contribution to nighttime aerosol formation in regions that are both biogenically- and anthropogenically-influenced. This work seeks to characterize the role of each competing nighttime oxidant over this broader range of monoterpenes and the influence of each on SOA formation.

2 Methods

SOA formation experiments were performed in a darkened 400 L PFA film chamber, shown in Fig. 2, run in flow-through mode with precursors added continuously. Each experiment, as described in Table 2, measured the aerosol production from a single monoterpene oxidized by O_3 with varying concentrations of NO_2 added. In order to make comparisons across both the range of monoterpenes and the range of [NO_2], the monoterpene source and O_3 source concentrations were kept as constant as possible throughout the full study, allowing only the identity of the BVOC and the concentration of NO_2 to vary.

O_3 (and NO_2, when applicable) were introduced into the chamber first and allowed to reach steady state prior to initiation of each experiment by BVOC injection. O_3 was generated by flowing zero air (Sabio Model 1001 compressed zero air generator) through a flask containing a Pen-Ray Hg lamp (primary energy at 254 nm) and was continually measured from the outlet of the chamber using a Dasibi Model 1003-AH O_3 monitor.

ACPD
15, 14923–14960, 2015

NO_2 was introduced from a calibrated cylinder (Air Liquide, 0.3 % by volume in N_2), and monitored using a Thermo Model 17i chemiluminescence NO_x/NH_3 analyzer. Chemiluminescence NO_x analyzers are sensitive to any species that is converted to NO in the 350 °C Mb converter responsible for converting NO_2 to NO (Winer et al., 1974; Grosjean and Harrison, 1985). Some of these additional species include N_2O_5, peroxynitrates (PNs), and alkyl-nitrates (ANs). At the high concentrations used in this study, these NO_y contributions were significant. Kinetics modeling of the oxidant stabilization period (described in the Supplement), corroborated by a characterization of oxidant stabilization using chemiluminescence NO_x analyzers and a cavity ringdown spectrometer sensitive only to NO_2, indicates that we detected N_2O_5 with approximately unit efficiency in the NO_2 channel of the Thermo NO_x analyzer. The sensitivity of this NO_x analyzer to PNs and ANs, which would have formed following BVOC addition, was not calibrated, but is expected to be near unity based on previous studies (Winer et al., 1974; Grosjean and Harrison, 1985). Modeling only the oxidant stabilization period, where NO_2 and N_2O_5 were likely the only species detected in the NO_2 channel, provided the initial NO_2 concentrations shown in Table 2.

Once the oxidants stabilized, BVOC was introduced by flowing zero air over a small, cooled liquid sample of the target BVOC ((1R)-(+)-alpha-Pinene, TCI America, > 95.0 %; (−)-beta-Pinene, TCI America, > 94 %; (+)-3-Carene, TCI America, > 90.0 %; (R)-(+)-Limonene, Aldrich, > 97 %). The chiller temperature was held constant (±0.3 °C) during a single experiment, and ranged from −27 to −21 °C for the different monoterpenes, based on the temperature-dependent vapor pressure that is calculated to give a mixing ratio of approximately 100 ppm in the source flask (Fig. S.3) (Haynes et al., 2012). Since vapor pressure data was unavailable for Δ^3-carene, it was estimated to reach the temperature-dependent vapor pressure at −25 °C – between α-pinene and β-pinene's target temperatures – due to structural similarities.

Since experiments were initiated by introducing BVOC into an oxidant-rich chamber, online measurement of the reaction of the BVOC was not possible. Instead, initial VOC concentrations were characterized directly from the source flask before and after each

ACPD
15, 14923–14960, 2015

experiment using a SRI Model 8610C gas chromatograph with flame ionization detector (GC-FID). Source concentrations were somewhat variable over time, so BVOC was also modeled independent of measurements in order to verify initial concentrations listed in Table 2. Methodology and uncertainties are described in the Supplement.

In addition to measurements of the gas-phase precursors, two methods were employed to measure the resulting aerosol loading and composition. Particle size distributions between 20 and 800 nm were measured at 85 s time resolution with a Scanning Electrical Mobility Sizer (SEMS; BMI Model 2002) consisting of a differential mobility analyzer (BMI Model 2000C) coupled to a Water Condensation Particle Counter (TSI Model 3781). Size-dependent aerosol loss rates to the chamber walls were characterized and used to correct size distributions to reflect the total aerosol number and volume concentrations produced in each experiment (McMurry and Grosjean, 1985; VanReken et al., 2006; Fry et al., 2014). This methodology is described in further detail in the Supplement. Aerosol samples from each experiment were collected onto filters (47 mm quartz fiber). Each filter was extracted by sonication in 3 : 1 deionized water : acetonitrile to minimize solvent reactions with analyte compounds (Bateman et al., 2008), and the resulting extract was analyzed offline by High Performance Liquid Chromatography-Electrospray Ionization-Mass Spectrometry (HPLC-ESI-MS).

Due to its relatively soft ionization source and thus minimal fragmentation of analyte compounds, ESI-MS has been employed in several studies to probe SOA composition (Bateman et al., 2008, 2012; Walser et al., 2008; Doezema et al., 2012). The HPLC-ESI-MS system used here consists of an Agilent 1100 Series liquid chromatograph coupled to an Agilent LC/MCD TOF G1969A time-of-flight mass spectrometer with an electrospray ionization source. The chromatographic separation occurred on a Kinetex 100 mm × 3 mm C18 column with 2.6 µm particle size and a sample injection volume of 50 µL at a flow rate of 0.5 mL min^{-1}. The electrospray ionization system had a nebulizer gas pressure of 50 psi and an electrospray voltage of 3000 V. High mass resolution ($m/\Delta m$ varies between 5000 at m/z 118 amu to 15 000 at m/z 1822 amu) and

ACPD
15, 14923–14960, 2015

chromatographic separation of the analytes allowed for straightforward identification of product molecular formulae (Desyaterik et al., 2013).

3 Results and discussion

3.1 Aerosol formation trends

Raw number and volume concentration time series are presented in Fig. 3. These comparisons are not directly indicative of relative yields due to differences in initial monoterpene concentrations shown in Table 2 (see Sect. 3.2 for true aerosol mass yields). However, they nicely illustrate the vast diversity of the behavior of each monoterpene with respect to systematically changing oxidant conditions, from O_3-dominated to NO_3-dominated. α-pinene exhibits a decrease in both the total number of particles produced (N_{tot}) and total aerosol volume produced (V_{tot}) with increasing NO_2, consistent with the findings of other studies (Perraud et al., 2012; Presto et al., 2005). β-pinene and Δ^3-carene both exhibit a similar decrease in N_{tot} with addition of NO_2 as α-pinene, but at early times in the reaction, the addition of NO_2 appears to enhance volume growth relative to the O_3-only experiment. Limonene exhibits enhancement in both N_{tot} and V_{tot}. While all three of the monoalkene monoterpenes produce fewer particles at higher [NO_2], α-pinene is the only terpene for which the aerosol production seems to be systematically depleted with the addition of NO_2. β-pinene and Δ^3-carene, in contrast, seem to level off at comparable N_{tot} values for the intermediate range of [NO_2]. All four monoterpenes exhibit suppression of aerosol formation at the highest [NO_2] studied, which may be the result of $RO_2 + NO_2$ chemistry becoming kinetically dominant at such high concentrations and producing metastable, less condensable peroxynitrate products (Barthelmie and Pryor, 1999).

ACPD
15, 14923–14960, 2015

3.2 SOA yields

Unitless aerosol mass yields (Y) are defined as the aerosol mass produced per hydrocarbon mass consumed ($Y = \Delta M/\Delta\mathrm{HC}$). Since the hydrocarbon was not measured online during experiments, ΔHC values were determined using the gas-phase kinetics model described in detail in the Supplement. The modeled cumulative concentration of monoterpene reacted was converted to ΔHC in μg m^{-3} using the molecular weight of monoterpenes (136.23 g mol^{-1}). ΔM was determined by converting the wall loss-corrected aerosol total volume data to mass, assuming a SOA density of 1.4 g mL^{-1} (Hoyle et al., 2011). Thus a time series of mass yields was attainable, shown in Fig. 4 as aerosol mass produced (ΔM) vs. ΔHC consumed, where ΔM and ΔHC are calculated relative to the beginning of the experiment. In the kinetics model, ΔHC is calculated based on how much of each oxidant reacts with the monoterpene. However, NO_3 can also react with subsequent RO_2 radicals, thus depleting the concentration available to react directly with BVOC. The rate constant for $RO_2 + NO_3$ (2×10^{-12} cm^3 $molec^{-1}$ s^{-1}) is reasonably well known and constant over a range of RO_2 structures (Vaughan et al., 2006). The rate constant for $RO_2 + RO_2$, the main competing RO_2 sink, is far more variable over RO_2 structures, though, so the "best estimate" employed in this study spans three orders of magnitude (described further in Supplement). Therefore, $k_{RO_2+RO_2}$ is the largest source of uncertainty in ΔHC, and aerosol yield ranges are calculated spanning the minimum (10^{-15} cm^3 $molec^{-1}$ s^{-1}) and maximum (10^{-12} cm^3 $molec^{-1}$ s^{-1}) values used. Because O_3 is not expected to react with RO_2 (whereas NO_3 does), ΔHC from the O_3-only experiments does not vary in response to shifting $k_{RO_2+RO_2}$ values. Aerosol yields were not constant over the course of each experiment, as seen by the non-linear yield curves in Fig. 4, where the regions with the greatest slopes (relative to ΔHC = 0) have the highest mass yield. The yields reported in Table 3 are the maximum yield observed during the course of the experiment, typically observed during the first two hours, for each of the low and high $k_{RO_2+RO_2}$ limits. In some cases, the aerosol growth rapidly exceeded the size range of the SEMS (20–800 nm). Aerosol

ACPD
15, 14923–14960, 2015

data presented here is truncated as soon as the size distribution exceeds the range of the SEMS instrument and is represented as a lower limit to the maximum aerosol yield because all subsequent data will be an underestimation of mass.

With the mass yield effectively normalizing these mass yields across varying ΔHC, we still see similar trends as were observed in the V_{tot} panels of Fig. 3. Figure 4 and Table 3 illustrate that increasing [NO_2] substantially depletes aerosol formation from α-pinene, whereas β-pinene and Δ^3-carene have comparable yields over the full range of oxidant conditions, and limonene exhibits enhancement of aerosol formation at higher [NO_2]. It should be noted that yield calculations were only performed on the O_3-only and lowest two [NO_2] studied for each monoterpene due to difficulties in reliably reproducing ΔHC in the kinetics model for the highest [NO_2] experiments.

3.3 Individual oxidant contributions

Gas-phase kinetics modeling of the steady state conditions in the chamber yielded the time series of relative O_3 and NO_3 (and OH) contributions to BVOC oxidation. Since each experiment starts with O_3, NO_2, NO_3, and N_2O_5 at their equilibrium concentrations, initial BVOC oxidation will be dominated by NO_3, which reacts orders of magnitude faster than O_3 (Table 1). Eventually, as concentrations of precursors change over time, rates to each oxidant change and O_3 starts to contribute. We also assume OH is produced from stabilized Criegee intermediates from ozonolysis according to the monoterpene-dependent yields found in Atkinson et al. (1992) and described in the Supplement. The timing and relative contribution of O_3 depends on the relative rate constants of O_3 and NO_3 with each monoterpene, and thus the influence of each oxidant varies for all conditions tested.

For α-pinene, the window where NO_3 is responsible for all oxidation is relatively short (< 30 min for either NO_2 experiment). In general, it can be assumed that any aerosol formed in a period dominated by a single oxidant is the aerosol yield of that BVOC/oxidant combination. Therefore, this period where NO_3 is responsible for all oxidation should give the NO_3 + α-pinene aerosol yield. It is especially notable in all of

ACPD
15, 14923–14960, 2015

the α-pinene experiments that no aerosol forms until O_3 starts contributing, as seen in Fig. 5. This observation is consistent with several studies that have seen low or even 0 % aerosol yields for α-pinene + NO_3 (Hallquist et al., 1999; Spittler et al., 2006; Fry et al., 2014). Because NO_3 gives approximately 0 % aerosol yield, any aerosol produced from α-pinene can be assumed to come from O_3 (and OH) oxidation. We can calculate the O_3 (with OH) aerosol yield in the NO_2-influenced experiments using $\Delta M/\Delta HC_{O_3+OH}$, where any of the BVOC reacted by NO_3 is excluded from the yield calculation. In the O_3-only experiment, α-pinene has a 28 % mass yield. The lowest NO_2 condition has a 16–28 % yield from O_3 (+ OH), which is consistent with the 28 % yield from the O_3-only experiment. At the next highest [NO_2], the O_3 yield drops to 2–4 %, which may simply be explained by having the lowest background aerosol mass and thus smaller absorptive partitioning contributions (Pankow, 1994).

β-pinene in general produced the least aerosol mass and lowest number concentrations. Due to the very small number concentrations but modest aerosol yields (and thus abundant condensable vapors to grow the small number of particles), β-pinene size distributions grew above the size range of the SEMS quite rapidly during the NO_2 experiments. The relatively short span of aerosol data, combined with faster loss of O_3 to reaction with NO_2 than to β-pinene oxidation (Table 1), resulted in the entire period of observable aerosol formation being dominated by NO_3 oxidation at all concentrations of NO_2. The two lowest concentrations of NO_2 both had yields within a range of 8–14 %, further indicating that both experiments were dominated by NO_3 oxidation rather than varying contributions from NO_3 and O_3. Δ^3-carene displayed similar behavior to β-pinene. Most, though not all, of the oxidation during aerosol production went by NO_3. In the two lowest NO_2 concentration experiments, the maximum aerosol yield during the period only influenced by NO_3 oxidation was approximately 12–21 %. Limonene maintained relatively high aerosol yields from each set of oxidation conditions, indicating high aerosol yields from both O_3 and NO_3 oxidation. For the lowest [NO_2], the first 30 min of BVOC oxidation was dominated by NO_3, with a 36–42 % yield.

ACPD
15, 14923–14960, 2015

During these periods of exclusively NO_3 oxidation, the relative aerosol yields for each monoterpene follow the same trend observed in Fry et al. (2014), which measured aerosol yields from NO_3 oxidation alone at lower initial concentrations of both BVOC and NO_3 and observed α-pinene $\approx 0 < \beta$-pinene $< \Delta^3$-carene $<$ limonene. This consistency further stresses the importance of individual oxidant contributions in this complex system. The percentage of BVOC reacted by each of the three oxidants was modeled and is shown in Table 4. Comparisons were made at two hours into the reaction after the initial buildup of NO_3 and N_2O_5 was depleted and chemical production of NO_3 more realistically competes with O_3 oxidation of BVOCs. Even at this point in time, NO_3 dominates the initial oxidation pathway for all NO_2 concentrations and all monoterpenes.

3.4 Determination of dominant nighttime oxidant using NO_2 to BVOC ratio

Using literature rate constant data (Table 1), we can approximate the NO_2 / BVOC mixing ratio regime where NO_3 will dominate nighttime oxidation for each monoterpene. Since O_3 contributes to both NO_3 formation and BVOC oxidation, and for all monoterpenes NO_3 oxidation is much faster than O_3 oxidation, we assume that once NO_3 production becomes faster than O_3 oxidation of BVOC (Eq. 1), NO_3 becomes the dominant oxidant. The ratio of NO_2 / BVOC at which this crossover occurs, defined in Eq. (2), is calculated for each monoterpene and reported in Table 5.

$$k_{(O_3+NO_2)}[O_3][NO_2] > k_{(O_3+BVOC)}[O_3][BVOC] \quad (1)$$

$$\frac{[NO_2]}{[BVOC]} > \frac{k_{(O_3+BVOC)}}{k_{(O_3+NO_2)}} \quad (2)$$

This calculation leaves out factors like competing sinks for NO_3 and is thus a very crude approximation. Nevertheless, it is noteworthy how small the magnitude of these ratios are. During the 2011 BEACHON-RoMBAS field campaign, which took place in a relatively remote forested location in the Rocky Mountain front range, $[NO_2]$ typ-

ACPD
15, 14923–14960, 2015

ically peaked at night around 2 ppb, and total monoterpene concentrations (1 : 1 : 1 α-pinene : β-pinene : Δ^3-carene) peaked at night around 0.6 ppb (Fry et al., 2013). Assuming 0.2 ppb from each of the speciated monoterpenes, that gives $[NO_2]$ / [BVOC] ratios of 10 for each – well above the minimum values presented in Table 5. These ratios are expected to be substantially higher in regions with stronger anthropogenic influences. This analysis suggests that NO_3 is not only a relevant contributor to nighttime oxidation chemistry, it may actually dominate oxidation pathways in many regions.

3.5 Bulk SOA composition

Filter samples from experiments that yielded sufficient aerosol mass (all expts in Table 2 except 1, 5, 9, 13) were collected and analyzed offline by HPLC-ESI-MS at Colorado State University. Because electrospray ionization is a soft ionization technique, this method has been shown to be especially useful for detecting a wide range of m/z products – including oligomer species that are likely to be significant SOA constituents (Walser et al., 2008; Surratt et al., 2006; Doezema et al., 2012). Although quantitative comparisons of products are not possible due to differences in mass loadings and a lack of calibration standards, qualitative differences in product distributions were readily apparent and consistent with observed aerosol yield trends.

Introducing NO_2 into ozonolysis of monoterpenes influences the composition of resulting SOA in two different ways: first, by forming NO_3 that can either oxidize BVOC directly or react with NO_3- or O_3-initiated RO_2, or second, by directly reacting with RO_2 or other products and reaction intermediates as NO_2. A visual comparison of the total ion chromatograms from ozonolysis of β-pinene with no NO_2 and the two lowest concentrations of NO_2 (Fig. 6) shows that several new products form once NO_2 is added, and that in general increasing $[NO_2]$ simply increases the intensity of those products rather than changing product identities substantially. For ease of interpretation, results from all of the NO_2-containing experiments were combined into a single product distribution from "NO_3-influenced oxidation." We can then compare those product distributions to those of the O_3-only experiments. A complete list of compound formulae detected

ACPD
15, 14923–14960, 2015

(> 1.5 % relative intensity, see Supplement) in the O_3 and NO_3 dominated oxidation of each monoterpene is compiled in Table S.2.

To best highlight qualitative differences in the identity of molecules that make SOA for each set of precursors, every unique compound (distinct either in mass, retention time, or both) was accounted for once, not normalized by peak intensity. A variety of average bulk composition parameters were calculated for each experiment, highlighted in Table 6, including average number of C, O, and N atoms per compound, molecular weight, and total number of products. Some artifacts may remain in this dataset, such as impurities not captured by the background subtraction or product fragments that do not reflect the original identity of the SOA product. The former should affect all samples uniformly in this analysis and thus will not influence qualitative comparisons, and the latter will either affect multiple samples and thus be irrelevant in comparisons or only affect single samples and thus still provide interesting qualitative differences.

A direct correlation between any of the average parameters (MW_{avg}, C_{avg}, O_{avg}, N_{avg}) in Table 6 and absolute aerosol yields is not obvious. Limonene ozonolysis, for example, produced the highest aerosol mass of all the conditions tested, but its average MW and number of C or O atoms are comparable to ozonolysis from all the other monoterpenes, and substantially lower than any of the NO_3 experiments. However, the difference in average values, defined as the difference in each average parameter between O_3 and NO_3 dominated oxidation for each monoterpene (Δ_{avg}), are consistent with O_3 vs. NO_3 yield comparisons. β-pinene and Δ^3-carene have similar Δ_{avg} values for each parameter (as well as similar absolute values for each oxidant condition), suggesting that the addition of NO_3 affects the product distribution of these two monoterpenes similarly. The Δ_{avg} values for limonene are much higher than any other monoterpene in this study, consistent with it having the highest NO_3 aerosol yields. Again, perhaps most notably, the Δ_{avg} parameters hover near zero for α-pinene, suggesting that the aerosol composition does not differ much between the two oxidants – consistent with all of α-pinene's aerosol production coming exclusively from O_3-oxidation.

ACPD
15, 14923–14960, 2015

To illustrate some of the finer detail of these product distributions, Fig. 7 shows histograms where each observed product is binned by compound mass, in 50 amu intervals. Every experiment shows some contribution from oligomer products ($m/z > 246$, according to Perraud et al., 2010, > 300 according to Walser et al., 2008), but this contribution is most pronounced from NO_3 oxidation of β-pinene, Δ^3-carene, and limonene. In particular, we observe substantially more distinct products > 400 amu from β-pinene, Δ^3-carene, and limonene with the $O_3/NO_2/NO_3$ mixture than from O_3 alone. In this region, the mass distributions for α-pinene in both oxidant conditions are identical. Since mass is an important contributing factor to volatility (e.g. Donahue et al., 2011), these high mass products are likely important in aerosol formation and growth, and thus may be explanatory of the observed yield differences from NO_3-oxidation. If oligomerization is an important pathway leading to SOA formation and growth from NO_3-initiated chemistry, α-pinene's lack of oligomer products with NO_3 may be responsible for its 0 % aerosol yield. In contrast, comparison of the four O_3-only histograms shows relatively small contributions of high MW oligomers for any monoterpene, in spite of quite high aerosol yields in some cases, indicating that aerosol formation by ozonolysis may not require oligomerization.

Recent studies of SOA nucleation and growth from ozonolysis of α-pinene have shown that highly oxidized and/or oligomeric species are likely important in nucleation and early growth, but that growth beginning around 20 nm is dominated by lower MW products (140–380 amu) (Zhao et al., 2013; Winkler et al., 2012). This latter MW range is consistent with the ozonolysis products we observe for all four monoterpenes, indicating that high MW products may dominate only early stages of growth and are thus not detectable at the high mass loadings in this study. NO_3 oxidation, on the other hand, seems to provide a weaker source of low volatility compounds contributing to nucleation and early growth, as seen in the decrease of N_{tot} with increasing $[NO_2]$ in Fig. 3 (with the exception of limonene), but produces oligomers throughout the full time period of aerosol growth, leading to total aerosol mass concentrations that rival ozonolysis (with the exception of α-pinene), as seen in Fig. 4. Further supporting this observed differ-

ACPD
15, 14923–14960, 2015

ence in products from ozonolysis compared to NO_3 oxidation is the difference in the reaction rate of each process. O_3 + BVOC is much slower than NO_3 + BVOC, which means that RO_2 is produced more slowly from ozonolysis and thus the RO_2 lifetime is much longer with respect to other radical species. Longer RO_2 lifetimes are more conducive to isomerization processes like autoxidation (Crounse et al., 2013; Jokinen et al., 2014), which may be responsible for the initial high MW nucleating species observed in other ozonolysis studies. In contrast, NO_3 oxidation produces RO_2 much more rapidly, therefore increasing the likelihood of $RO_2 + RO_2$ oligomerization.

Mass spectra alone provide limited compositional information since they do not distinguish between different functional groups. However, in this system, one functional group that can be easily parsed out of the data is the nitrate group. From the NO_3 initiated oxidation chemistry, we expect that any nitrogen present in a molecule is a part of a nitrate functional group. (Some instances of –NO and –ONO have been found in the compound list, causing relatively high N_{avg} values for α-pinene + O_3, for example, where we expect any nitrogen is due to impurities.) The Δ_{avg} values in Table 6 for N_{avg} provide an approximate estimate of relative aerosol organic nitrate yield. β-pinene, Δ^3-carene, and limonene all exhibit a substantial increase in average number of N per molecule with the addition of NO_2, consistent with the relatively high organic nitrate yields observed from NO_3 oxidation of those species in other studies (Fry et al., 2014; Hallquist et al., 1999). α-pinene produces comparatively fewer nitrogen-containing SOA products in the presence of NO_2. While the organic nitrate products from α-pinene may be relatively volatile and thus not partition appreciably into the aerosol phase, it is clear that this is not a universal characteristic of C_{10} organic nitrates, as many do partition into the aerosol phase for all three other monoterpenes studied – even those with relatively low total aerosol mass loading.

We note that the products observed here from ozonolysis vs. NO_3 oxidation are consistent with proposed mechanisms in the literature. Table S.3 includes proposed structures for several masses that have been observed in other studies, including several monomeric carboxylic acids and aldehydes from ozonolysis (Glasius et al., 2000; Yu

ACPD
15, 14923–14960, 2015

et al., 1999) as well as multi-functional monomeric nitrates from NO_3-oxidation (Wangberg et al., 1997; Perraud et al., 2010), some of which have been included in Fig. 6 to highlight relative intensities across different NO_2 conditions. Several more speculative structures are shown in the Supplement to indicate that observed oligomeric masses can be reasonably achieved from dimers of first generation oxidation products.

4 Conclusions

This work adds to the growing body of monoterpene aerosol yield comparison literature suggesting that monoterpene oxidation has widely varying aerosol yields depending on the specific monoterpene and oxidant combination (Fry et al., 2014; Griffin et al., 1999; Hallquist et al., 1999; Ng et al., 2006; Glasius et al., 2000; Yu et al., 1999; Lee et al., 2006). We therefore conclude, first and foremost, that there is no single "representative" monoterpene. Furthermore, the monoterpene most often considered representative of BVOC oxidation, α-pinene, presents here as the greatest anomaly with respect to aerosol formation, showing higher ozonolysis aerosol mass yields than even limonene, and showing 0 % aerosol yields from reaction with NO_3.

We show that under the influence of NO_3, α-pinene produces comparatively few organic nitrates and oligomers relative to the other three monoterpenes studied. This finding is consistent with α-pinene's negligible aerosol yield with NO_3 and also suggests more generally that oligomers and potentially organic nitrate monomers are important products leading to SOA formation from NO_3. Additionally, the difference in product distributions between O_3 and NO_3 oxidation for all monoterpenes studied (except α-pinene) indicates that each oxidant broadly employs a different mechanism toward condensable products – where O_3 likely nucleates and grows enough aerosol mass early in the reaction that subsequent condensation is governed by comparatively small molecular weight species, whereas NO_3 produces less extremely low volatility material early but produces oligomers consistently throughout the period of condensation such that they constitute an observable fraction of the bulk aerosol.

ACPD
15, 14923–14960, 2015

Careful treatment of the first generation kinetics of this atmospherically relevant nighttime oxidant mixture also served to contextualize the relative importance of each observed aerosol precursor in different regions. We propose using NO_2 / BVOC ratios for each monoterpene to predict the dominant nighttime oxidation pathway for each (Table 5). For example, for β-pinene at NO_2 / BVOC ratios greater than 0.47, NO_3 oxidation will begin to out-compete O_3 oxidation, suggesting that β-pinene oxidation by O_3 is likely to be minor at night in all but the most pristine environments. β-pinene displays a rather extreme manifestation of this observation, but all four monoterpenes studied have NO_2 / BVOC ratios such that NO_3 oxidation is likely to dominate even in relatively remote regions.

The complexity shown by just these four BVOCs reacting with two different oxidants suggests that bulk parameters in global and regional models need to be very carefully considered if they are going to accurately match observed ambient organic aerosol loadings. These models use one or two, typically daytime, aerosol yield parameters for bulk monoterpenes – often considering α-pinene or β-pinene yields to be representative (e.g. Lane et al., 2008). To the knowledge of the authors, the modeling approach of Pye et al. (2010) is the only global-scale model that parameterizes NO_3 chemistry. Future challenges in constraining the global aerosol budget will likely require creating more nuanced approaches to modeling different regions with ostensibly similar chemistry that has been shown to have diverse effects on aerosol formation.

The Supplement related to this article is available online at doi:10.5194/acpd-15-14923-2015-supplement.

Acknowledgements. J. L. Fry and D. C. Draper gratefully acknowledge funding from the National Center for Environmental Research (NCER) STAR Program, EPA#RD-83539901 as well as the Reed College Class of '21 Award. In addition, we thank Rhiana Meade for development of the RECv1.0 as well as Dean Atkinson for donation of PFA film to build the RECv2.0 used

ACPD
15, 14923–14960, 2015

in this study. D. K. Farmer acknowledges the National Science Foundation (AGS 1240611) for support.

References

Atkinson, R. and Arey, J.: Atmospheric degradation of volatile organic compounds, Chem. Rev., 103, 4605–4638, doi:10.1021/cr0206420, 2003. 14948

Atkinson, R., Aschmann, S. M., Arey, J., and Shorees, B.: Formation of OH radicals in the gas phase reactions of O_3 with a series of terpenes, J. Geophys. Res.-Atmos., 97, 6065–6073, doi:10.1029/92JD00062, 1992. 14932, 14951

Ayres, B. R., Allen, H. M., Draper, D. C., Brown, S. S., Jimenez, J. L., Day, D. A., De Gouw, J., Cohen, R. C., Baumann, K., Takahama, S., Thornton, J. A., Goldstein, A. H., and Fry, J. L.: NO_y fate at SOAS 2013: organic nitrate aerosol formation via NO_3 + BVOC and comparison to inorganic nitrate aerosol, submitted, 2015. 14926

Barthelmie, R. J. and Pryor, S. C.: A model mechanism to describe oxidation of monoterpenes leading to secondary organic aerosol: 1. α-pinene and β-pinene, J. Geophys. Res.-Atmos., 104, 23657–23699, doi:10.1029/1999JD900382, 1999. 14930

Bateman, A. P., Walser, M. L., Desyaterik, Y., Laskin, J., Laskin, A., and Nizkorodov, S. A.: The effect of solvent on the analysis of secondary organic aerosol using electrospray ionization mass spectrometry, Environ. Sci. Technol., 42, 7341–7346, doi:10.1021/es801226w, 2008. 14929

Bateman, A. P., Laskin, J., Laskin, A., and Nizkorodov, S. A.: Applications of high-resolution electrospray ionization mass spectrometry to measurements of average oxygen to carbon ratios in secondary organic aerosols, Environ. Sci. Technol., 46, 8315–8324, doi:10.1021/es3017254, 2012. 14929

Boyd, C. M., Sanchez, J., Xu, L., Eugene, A. J., Nah, T., Tuet, W. Y., Guzman, M. I., and Ng, N. L.: Secondary Organic Aerosol (SOA) formation from the β-pinene + NO_3 system: effect of humidity and peroxy radical fate, Atmos. Chem. Phys. Discuss., 15, 2679–2744, doi:10.5194/acpd-15-2679-2015, 2015. 14926

Carlton, A. G., Pinder, R. W., Bhave, P. V., and Pouliot, G. A.: To what extent can biogenic SOA be controlled?, Environ. Sci. Technol., 44, 3376–3380, doi:10.1021/es903506b, 2010. 14926

ACPD
15, 14923–14960, 2015

Crounse, J. D., Nielsen, L. B., Jørgensen, S., Kjaergaard, H. G., and Wennberg, P. O.: Autoxidation of organic compounds in the atmosphere, J. Phys. Chem. Lett., 4, 3513–3520, doi:10.1021/jz4019207, 2013. 14938

Davidson, C. I., Phalen, R. F., and Solomon, P. A.: Airborne particulate matter and human health: a review, Aerosol Sci. Tech., 39, 737–749, doi:10.1080/02786820500191348, 2005. 14925

Desyaterik, Y., Sun, Y., Shen, X., Lee, T., Wang, X., Wang, T., and Collett, J. L.: Speciation of "brown" carbon in cloud water impacted by agricultural biomass burning in eastern China, J. Geophys. Res.-Atmos., 118, 7389–7399, doi:10.1002/jgrd.50561, 2013. 14930

Doezema, L. A., Longin, T., Cody, W., Perraud, V., Dawson, M. L., Ezell, M. J., Greaves, J., Johnson, K. R., and Finlayson-Pitts, B. J.: Analysis of secondary organic aerosols in air using extractive electrospray ionization mass spectrometry (EESI-MS), RSC Adv., 2, 2930–2938, doi:10.1039/C2RA00961G, 2012. 14929, 14935

Donahue, N. M., Epstein, S. A., Pandis, S. N., and Robinson, A. L.: A two-dimensional volatility basis set: 1. organic-aerosol mixing thermodynamics, Atmos. Chem. Phys., 11, 3303–3318, doi:10.5194/acp-11-3303-2011, 2011. 14937

Ehn, M., Thornton, J. A., Kleist, E., Sipila, M., Junninen, H., Pullinen, I., Springer, M., Rubach, F., Tillmann, R., Lee, B., Lopez-Hilfiker, F., Andres, S., Acir, I.-H., Rissanen, M., Jokinen, T., Schobesberger, S., Kangasluoma, J., Kontkanen, J., Nieminen, T., Kurten, T., Nielsen, L. B., Jorgensen, S., Kjaergaard, H. G., Canagaratna, M., Maso, M. D., Berndt, T., Petaja, T., Wahner, A., Kerminen, V.-M., Kulmala, M., Worsnop, D. R., Wildt, J., and Mentel, T. F.: A large source of low-volatility secondary organic aerosol, Nature, 506, 476–479, doi:10.1038/nature13032, 2014. 14925

Fry, J. L., Kiendler-Scharr, A., Rollins, A. W., Wooldridge, P. J., Brown, S. S., Fuchs, H., Dubé, W., Mensah, A., dal Maso, M., Tillmann, R., Dorn, H.-P., Brauers, T., and Cohen, R. C.: Organic nitrate and secondary organic aerosol yield from NO_3 oxidation of β-pinene evaluated using a gas-phase kinetics/aerosol partitioning model, Atmos. Chem. Phys., 9, 1431–1449, doi:10.5194/acp-9-1431-2009, 2009. 14926

Fry, J. L., Kiendler-Scharr, A., Rollins, A. W., Brauers, T., Brown, S. S., Dorn, H.-P., Dubé, W. P., Fuchs, H., Mensah, A., Rohrer, F., Tillmann, R., Wahner, A., Wooldridge, P. J., and Cohen, R. C.: SOA from limonene: role of NO_3 in its generation and degradation, Atmos. Chem. Phys., 11, 3879–3894, doi:10.5194/acp-11-3879-2011, 2011. 14926

ACPD
15, 14923–14960, 2015

Fry, J. L., Draper, D. C., Zarzana, K. J., Campuzano-Jost, P., Day, D. A., Jimenez, J. L., Brown, S. S., Cohen, R. C., Kaser, L., Hansel, A., Cappellin, L., Karl, T., Hodzic Roux, A., Turnipseed, A., Cantrell, C., Lefer, B. L., and Grossberg, N.: Observations of gas- and aerosol-phase organic nitrates at BEACHON-RoMBAS 2011, Atmos. Chem. Phys., 13, 8585–8605, doi:10.5194/acp-13-8585-2013, 2013. 14926, 14935

Fry, J. L., Draper, D. C., Barsanti, K. C., Smith, J. N., Ortega, J., Winkler, P. M., Lawler, M. J., Brown, S. S., Edwards, P. M., Cohen, R. C., and Lee, L.: Secondary organic aerosol formation and organic nitrate yield from NO_3 oxidation of biogenic hydrocarbons, Environ. Sci. Technol., 48, 11944–11953, doi:10.1021/es502204x, 2014. 14926, 14927, 14929, 14933, 14934, 14938, 14939

Geron, C., Rasmussen, R., Arnts, R. R., and Guenther, A.: A review and synthesis of monoterpene speciation from forests in the United States, Atmos. Environ., 34, 1761–1781, doi:10.1016/S1352-2310(99)00364-7, 2000. 14925

Glasius, M., Lahaniati, M., Calogirou, A., Di Bella, D., Jensen, N. R., Hjorth, J., Kotzias, D., and Larsen, B. R.: Carboxylic acids in secondary aerosols from oxidation of cyclic monoterpenes by ozone, Environ. Sci. Technol., 34, 1001–1010, doi:10.1021/es990445r, 2000. 14938, 14939

Goldstein, A. H. and Galbally, I. E.: Known and unexplored organic constituents in the Earth's atmosphere, Environ. Sci. Technol., 41, 1514–1521, doi:10.1021/es072476p, 2007. 14925

Griffin, R. J., Cocker, D. R., Flagan, R. C., and Seinfeld, J. H.: Organic aerosol formation from the oxidation of biogenic hydrocarbons, J. Geophys. Res.-Atmos., 104, 3555–3567, doi:10.1029/1998JD100049, 1999. 14925, 14926, 14939

Grosjean, D. and Harrison, J.: Response of chemiluminescence NO_x analyzers and ultraviolet ozone analyzers to organic air pollutants, Environ. Sci. Technol., 19, 862–865, doi:10.1021/es00139a016, 1985. 14928

Guenther, A., Hewitt, C. N., Erickson, D., Fall, R., Geron, C., Graedel, T., Harley, P., Klinger, L., Lerdau, M., Mckay, W. A., Pierce, T., Scholes, B., Steinbrecher, R., Tallamraju, R., Taylor, J., and Zimmerman, P.: A global model of natural volatile organic compound emissions, J. Geophys. Res.-Atmos., 100, 8873–8892, doi:10.1029/94JD02950, 1995. 14925

Hallquist, M., Wängberg, I., Ljungström, E., Barnes, I., and Becker, K.-H.: Aerosol and product yields from NO_3 radical-initiated oxidation of selected monoterpenes, Environ. Sci. Technol., 33, 553–559, doi:10.1021/es980292s, 1999. 14925, 14926, 14927, 14933, 14938, 14939

ACPD
15, 14923–14960, 2015

Hallquist, M., Wenger, J. C., Baltensperger, U., Rudich, Y., Simpson, D., Claeys, M., Dommen, J., Donahue, N. M., George, C., Goldstein, A. H., Hamilton, J. F., Herrmann, H., Hoffmann, T., Iinuma, Y., Jang, M., Jenkin, M. E., Jimenez, J. L., Kiendler-Scharr, A., Maenhaut, W., McFiggans, G., Mentel, Th. F., Monod, A., Prévôt, A. S. H., Seinfeld, J. H., Surratt, J. D., Szmigielski, R., and Wildt, J.: The formation, properties and impact of secondary organic aerosol: current and emerging issues, Atmos. Chem. Phys., 9, 5155–5236, doi:10.5194/acp-9-5155-2009, 2009. 14925

Haynes, W., Bruno, T. J., and Lide, D. R. (Eds.): CRC Handbook of Chemistry and Physics, 93rd edn. (internet version), CRC Press/Taylor and Francis, Boca Raton, FL, USA, 2012. 14928

Heald, C. L., Jacob, D. J., Park, R. J., Russell, L. M., Huebert, B. J., Seinfeld, J. H., Liao, H., and Weber, R. J.: A large organic aerosol source in the free troposphere missing from current models, Geophys. Res. Lett., 32, 4, doi:10.1029/2005GL023831, 2005. 14925

Heald, C. L., Coe, H., Jimenez, J. L., Weber, R. J., Bahreini, R., Middlebrook, A. M., Russell, L. M., Jolleys, M., Fu, T.-M., Allan, J. D., Bower, K. N., Capes, G., Crosier, J., Morgan, W. T., Robinson, N. H., Williams, P. I., Cubison, M. J., DeCarlo, P. F., and Dunlea, E. J.: Exploring the vertical profile of atmospheric organic aerosol: comparing 17 aircraft field campaigns with a global model, Atmos. Chem. Phys., 11, 12673–12696, doi:10.5194/acp-11-12673-2011, 2011. 14925

Hoyle, C. R., Boy, M., Donahue, N. M., Fry, J. L., Glasius, M., Guenther, A., Hallar, A. G., Huff Hartz, K., Petters, M. D., Petäjä, T., Rosenoern, T., and Sullivan, A. P.: A review of the anthropogenic influence on biogenic secondary organic aerosol, Atmos. Chem. Phys., 11, 321–343, doi:10.5194/acp-11-321-2011, 2011. 14925, 14931

IPCC: Climate Change 2013: The Physical Science Basis. Contribution of Working Group I to the Fifth Assessment Report of the Intergovernmental Panel on Climate Change, Cambridge University Press, Cambridge, UK and New York, NY, USA, doi:10.1017/CBO9781107415324, 2013. 14925

Jokinen, T., Sipilä, M., Richters, S., Kerminen, V.-M., Paasonen, P., Stratmann, F., Worsnop, D., Kulmala, M., Ehn, M., Herrmann, H., and Berndt, T.: Rapid autoxidation forms highly oxidized RO_2 radicals in the atmosphere, Angew. Chem. Int. Edit., 53, 14596–14600, doi:10.1002/anie.201408566, 2014. 14938

Kroll, J. H. and Seinfeld, J. H.: Chemistry of secondary organic aerosol: formation and evolution of low-volatility organics in the atmosphere, Atmos. Environ., 42, 3593–3624, doi:10.1016/j.atmosenv.2008.01.003, 2008. 14925

ACPD
15, 14923–14960, 2015

Lane, T. E., Donahue, N. M., and Pandis, S. N.: Effect of NO_x on secondary organic aerosol concentrations, Environ. Sci. Technol., 42, 6022–6027, doi:10.1021/es703225a, 2008. 14940
Lee, A., Goldstein, A. H., Kroll, J. H., Ng, N. L., Varutbangkul, V., Flagan, R. C., and Seinfeld, J. H.: Gas-phase products and secondary aerosol yields from the photooxidation of 16 different terpenes, J. Geophys. Res.-Atmos., 111, D17305, doi:10.1029/2006JD007050, 2006. 14939
McMurry, P. H. and Grosjean, D.: Gas and aerosol wall losses in Teflon film smog chambers, Environ. Sci. Technol., 19, 1176–1182, doi:10.1021/es00142a006, 1985. 14929
Middleton, P.: Sources of air pollutants, in: Composition, Chemistry, and Climate of the Atmosphere, edited by: Singh, H. B., Van Nostrand Reinhold, New York, 1995. 14925
Moldanova, J. and Ljungström, E.: Modelling of particle formation from NO_3 oxidation of selected monoterpenes, J. Aerosol Sci., 21, 1317–1333, doi:10.1016/S0021-8502(00)00041-0, 2000. 14926
Ng, N. L., Kroll, J. H., Keywood, M. D., Bahreini, R., Varutbangkul, V., Flagan, R. C., Seinfeld, J. H., Lee, A., and Goldstein, A. H.: Contribution of first- versus second-generation products to secondary organic aerosols formed in the oxidation of biogenic hydrocarbons, Environ. Sci. Technol., 40, 2283–2297, doi:10.1021/es052269u, 2006. 14925, 14926, 14939
Pankow, J.: An absorption-model of gas-particle partitioning of organic compounds in the atmosphere, Atmos. Environ., 28, 185–188, 1994. 14933
Perraud, V., Bruns, E. A., Ezell, M. J., Johnson, S. N., Greaves, J., and Finlayson-Pitts, B. J.: Identification of organic nitrates in the NO_3 radical initiated oxidation of α-pinene by atmospheric pressure chemical ionization mass spectrometry, Environ. Sci. Technol., 44, 5887–5893, doi:10.1021/es1005658, 2010. 14937, 14939
Perraud, V., Bruns, E. A., Ezell, M. J., Johnson, S. N., Yu, Y., Alexander, M. L., Zelenyuk, A., Imre, D., Chang, W. L., Dabdub, D., Pankow, J. F., and Finlayson-Pitts, B. J.: Nonequilibrium atmospheric secondary organic aerosol formation and growth, P. Natl. Acad. Sci. USA, 109, 2836–2841, doi:10.1073/pnas.1119909109, 2012. 14926, 14930
Pope III, C. A., Bates, D. V., and Raizenne, M. E.: Health effects of particulate air pollution: time for reassessment?, Environ. Health Persp., 103, 472–480, doi:10.2307/3432586, 1995. 14925
Presto, A. A., Huff Hartz, K. E., and Donahue, N. M.: Secondary organic aerosol production from terpene ozonolysis. 2. Effect of NO_x concentration, Environ. Sci. Technol., 39, 7046–7054, 2005. 14926, 14930

ACPD
15, 14923–14960, 2015

Pye, H. O. T., Chan, A. W. H., Barkley, M. P., and Seinfeld, J. H.: Global modeling of organic aerosol: the importance of reactive nitrogen (NO_x and NO_3), Atmos. Chem. Phys., 10, 11261–11276, doi:10.5194/acp-10-11261-2010, 2010. 14940

Reis, S., Pinder, R. W., Zhang, M., Lijie, G., and Sutton, M. A.: Reactive nitrogen in atmospheric emission inventories, Atmos. Chem. Phys., 9, 7657–7677, doi:10.5194/acp-9-7657-2009, 2009. 14926

Rollins, A. W., Browne, E. C., Min, K.-E., Pusede, S. E., Wooldridge, P. J., Gentner, D. R., Goldstein, A. H., Liu, S., Day, D. A., Russell, L. M., and Cohen, R. C.: Evidence for NO_x control over nighttime SOA formation, Science, 337, 1210–1212, doi:10.1126/science.1221520, 2012. 14926

Sakulyanontvittaya, T., Duhl, T., Wiedinmyer, C., Helmig, D., Matsunaga, S., Potosnak, M., Milford, J., and Guenther, A.: Monoterpene and sesquiterpene emission estimates for the United States, Environ. Sci. Technol., 42, 1623–1629, doi:10.1021/es702274e, 2008. 14925

Sander, S., Abbatt, J., Barker, J. R., Burkholder, J. B., Friedl, R. R., Golden, D. M., Huie, R. E., Kolb, C. E., Kurylo, M. J., Moortgat, G. K., Orkin, V. L., and Wine, P. H.: Chemical Kinetics and Photochemical Data for Use in Atmospheric Studies, Evaluation Number 17, JPL Publication, Jet Propulsion Laboratory, Pasadena, CA, USA, 10, 2011. 14948

Spittler, M., Barnes, I., Bejan, I., Brockmann, K., Benter, T., and Wirtz, K.: Reactions of NO_3 radicals with limonene and α-pinene: product and SOA formation, Atmos. Environ., 40, 116–127, doi:10.1016/j.atmosenv.2005.09.093, 2006. 14926, 14933

Surratt, J. D., Murphy, S. M., Kroll, J. H., Ng, N. L., Hildebrandt, L., Sorooshian, A., Szmigielski, R., Vermeylen, R., Maenhaut, W., Claeys, M., Flagan, R. C., and Seinfeld, J. H.: Chemical composition of secondary organic aerosol formed from the photooxidation of isoprene, J. Phys. Chem. A, 110, 9665–9690, doi:10.1021/jp061734m, 2006. 14935

VanReken, T. M., Greenberg, J. P., Harley, P. C., Guenther, A. B., and Smith, J. N.: Direct measurement of particle formation and growth from the oxidation of biogenic emissions, Atmos. Chem. Phys., 6, 4403–4413, doi:10.5194/acp-6-4403-2006, 2006. 14929

Vaughan, S., Canosa-Mas, C. E., Pfrang, C., Shallcross, D. E., Watson, L., and Wayne, R. P.: Kinetic studies of reactions of the nitrate radical (NO_3) with peroxy radicals (RO_2): an indirect source of OH at night?, Phys. Chem. Chem. Phys., 8, 3749–3760, doi:10.1039/B605569A, 2006. 14931

Walser, M. L., Desyaterik, Y., Laskin, J., Laskin, A., and Nizkorodov, S. A.: High-resolution mass spectrometric analysis of secondary organic aerosol produced by ozonation of limonene,

ACPD
15, 14923–14960, 2015

Phys. Chem. Chem. Phys., 10, 1009–1022, doi:10.1039/B712620D, 2008. 14929, 14935, 14937

Wangberg, I., Barnes, I., and Becker, K. H.: Product and mechanistic study of the reaction of NO_3 radicals with α-pinene, Environ. Sci. Technol., 31, 2130–2135, doi:10.1021/es960958n, 1997. 14939

Winer, A. M., Peters, J. W., Smith, J. P., and Pitts, J. N.: Response of commercial chemiluminescent nitric oxide-nitrogen dioxide analyzers to other nitrogen-containing compounds, Environ. Sci. Technol., 8, 1118–1121, doi:10.1021/es60098a004, 1974. 14928

Winkler, P. M., Ortega, J., Karl, T., Cappellin, L., Friedli, H. R., Barsanti, K., McMurry, P. H., and Smith, J. N.: Identification of the biogenic compounds responsible for size-dependent nanoparticle growth, Geophys. Res. Lett., 39, L20815, doi:10.1029/2012GL053253, 2012. 14937

Xu, L., Guo, H., Boyd, C. M., Klein, M., Bougiatioti, A., Cerully, K. M., Hite, J. R., Isaacman-VanWertz, G., Kreisberg, N. M., Knote, C., Olson, K., Koss, A., Goldstein, A. H., Hering, S. V., de Gouw, J., Baumann, K., Lee, S.-H., Nenes, A., Weber, R. J., and Ng, N. L.: Effects of anthropogenic emissions on aerosol formation from isoprene and monoterpenes in the southeastern United States, P. Natl. Acad. Sci., 112, 37–42, doi:10.1073/pnas.1417609112, 2015. 14926

Yu, J., Cocker, D., Griffin, R., Flagan, R., and Seinfeld, J.: Gas-phase ozone oxidation of monoterpenes: gaseous and particulate products, J. Atmos. Chem., 34, 207–258, 1999. 14927, 14938, 14939

Zhao, J., Ortega, J., Chen, M., McMurry, P. H., and Smith, J. N.: Dependence of particle nucleation and growth on high-molecular-weight gas-phase products during ozonolysis of α-pinene, Atmos. Chem. Phys., 13, 7631–7644, doi:10.5194/acp-13-7631-2013, 2013. 14937

ACPD
15, 14923–14960, 2015

Table 1. Rate constants at 298 K for $NO_2 + O_3$ (Sander et al., 2011) and for both O_3 and NO_3 with selected monoterpenes (Atkinson and Arey, 2003).

	$k \times 10^{17}$ (cm^3 $molec^{-1}$ s^{-1})	$k_{O_3} \times 10^{17}$ (cm^3 $molec^{-1}$ s^{-1})	$k_{NO_3} \times 10^{12}$ (cm^3 $molec^{-1}$ s^{-1})
$NO_2 + O_3$	3.2	–	–
α-pinene	–	8.4	6.2
β-pinene	–	1.5	2.51
Δ^3-carene	–	3.7	9.1
limonene	–	21	12.2

ACPD
15, 14923–14960, 2015

Table 2. Conditions for each chamber experiment.

Expt #	Date	$[BVOC]_i$[g] (ppb)	$[O_3]_i$ (ppb)	$[NO_2]_i$[g] (ppb)	RH (%)	Temp (K)	Notes
			α-pinene				
1	19 Dec 2012	780	485	–	33	294	f
2	5 Jan 2013	680	490	–	20	295	a
3	16 Jan 2013	590–715	480	510	24	294	a, c
4	18 Jan 2013	780–960	480	840	22	295	a, d
5	14 Jan 2013	~400	480	1400	22	294	b, e
			β-pinene				
6	7 Jan 2013	370	485	–	40	295	a
7	23 Jan 2013	470–680	480	530	23	295	a, c
8	25 Jan 2013	~500	480	910	40	295	a, b, d
9	21 Jan 2013	~700	480	2000	20	295	b, e
			Δ-carene				
10	9 Jan 2013	220	470	–	30	294	a
11	9 Mar 2013	250–340	470	290	27	295	a, c
12	13 Mar 2013	400–650	470	590	38	295	a, d
13	6 Feb 2013	~200	470	900	33	295	b, e
			limonene				
14	11 Jan 2013	470	485	–	20	295	a
15	23 Mar 2013	340–400	470	360	20	295	a, c
16	27 Mar 2013	470–560	470	720	31	295	a, d
17	21 Mar 2013	~400	465	1000	26	295	a, b, e

[a] SOA filter sample collected and analyzed by HPLC-ESI-MS.
[b] [BVOC] estimated by scaling available GC-FID data to modeled values, making these estimates more uncertain than others.
[c] Designated "low NO_2."
[d] Designated "medium NO_2."
[e] Designated "high NO_2."
[f] Experiment included to show reproducibility of chamber. Not included in analysis beyond Fig. 3.
[g] Values calculated using kinetics model.

ACPD
15, 14923–14960, 2015

Table 3. Maximum aerosol mass yield observed, typically occurring within the first two hours of each experiment. The ranges in the low and medium NO_2 experiments reflect uncertainty in ΔHC due to the $RO_2 + RO_2$ rate constant.

	Aerosol Mass Yield		
	O_3-only	low NO_2	med NO_2
α-pinene	28 %	6–7 %	0.7–0.8 %
β-pinene	16 %	≥ 10–14 %	≥ 8–12 %
Δ^3-carene	19 %	≥ 15–21 %	≥ 12–20 %
limonene	22 %	39–42 %	36–43 %

ACPD
15, 14923–14960, 2015

Table 4. Percentage of total BVOC reacted by each oxidant at 2 h into each experiment. In the model, OH is produced from Stabilized Criegee Intermediates from ozonolysis at the following ratios: α-pinene = 0.85; β-pinene = 0.35; Δ^3-carene = 1.06; limonene = 0.86 (Atkinson et al., 1992). Values from NO_2-containing experiments include two values expressed as *low (high)* where "low" denotes the lower $RO_2 + RO_2$ rate constant limit (10^{-15} cm^3 molec^{-1} s^{-1}), and "high" denotes the upper limit (10^{-12} cm^3 molec^{-1} s^{-1}) as described in the Supplement.

	$[NO_2]_i$ (ppb)	% by NO_3	% by O_3	% by OH
α-pinene	0	0	54	46
	510	44 (68)	34 (21)	22 (11)
	840	58 (78)	26 (15)	16 (7)
β-pinene	0	0	74	26
	530	77 (94)	18 (5)	5 (1)
	910	81 (95)	15 (4)	4 (1)
Δ^3-carene	0	0	49	51
	290	62 (92)	21 (5)	17 (3)
	590	63 (95)	20 (4)	17 (1)
limonene	0	0	54	46
	360	45 (74)	34 (18)	21 (8)
	720	59 (85)	26 (11)	15 (4)

ACPD
15, 14923–14960, 2015

Table 5. Minimum $[NO_2]$ / [BVOC] value reported for each monoterpene studied at which NO_3 is expected to dominate nighttime oxidation.

BVOC	$[NO_2]$ / [BVOC]
α-pinene	2.6
β-pinene	0.47
Δ^3-carene	1.2
limonene	6.6

ACPD
15, 14923–14960, 2015

Table 6. Average (± one SD) molecular weight, number of C, O, and N atoms, O / C, and total number of products identified by HPLC-ESI-MS analysis of aerosol collected from O_3 and NO_3 ($O_3 + NO_2 + NO_3$) oxidation of each monoterpene studied. The difference in average value for each parameter (Δ_{avg}) from each oxidation scheme was also tabulated for each monoterpene.

	α-pinene			β-pinene		
	O_3	NO_3	Δ_{avg}	O_3	NO_3	Δ_{avg}
MW_{avg}	237.6 ±86.9	233.9 ±81.0	−3.7	212.0 ±88.9	249.3 ±104.3	37.3
C_{avg}	13.8 ±5.4	13.2 ±5.0	−0.6	12.0 ±4.5	12.7±4.7	0.7
O_{avg}	2.9 ±1.6	3.1 ±1.7	0.2	2.9 ±2.1	4.2 ±2.6	1.3
N_{avg}	0.29 ±0.53	0.40 ±0.58	0.11	0.14 ±0.36	0.74 ±0.73	0.60
O / C	0.22 ±0.11	0.25 ±0.14	0.03	0.23 ±0.12	0.32 ±0.16	0.09
# ID'd	28	43	15	29	66	37
	Δ-carene			limonene		
MW_{avg}	191.7 ±56.9	232.1 ±111.5	40.4	216.9 ±81.2	306.5 ±128.6	89.6
C_{avg}	11.0 ±3.1	12.4 ±4.7	1.4	12.3 ±4.2	14.7 ±4.8	2.4
O_{avg}	2.4 ±1.2	3.6 ±3.0	1.2	2.9 ±1.8	5.9 ±4.0	3.0
N_{avg}	0.09 ±0.30	0.41 ±0.67	0.32	0.18 ±0.46	0.94 ±1.06	0.76
O / C	0.22 ±0.11	0.27 ±0.14	0.05	0.23 ±0.13	0.39 ±0.23	0.16
# ID'd	32	70	38	34	85	51

ACPD
15, 14923–14960, 2015

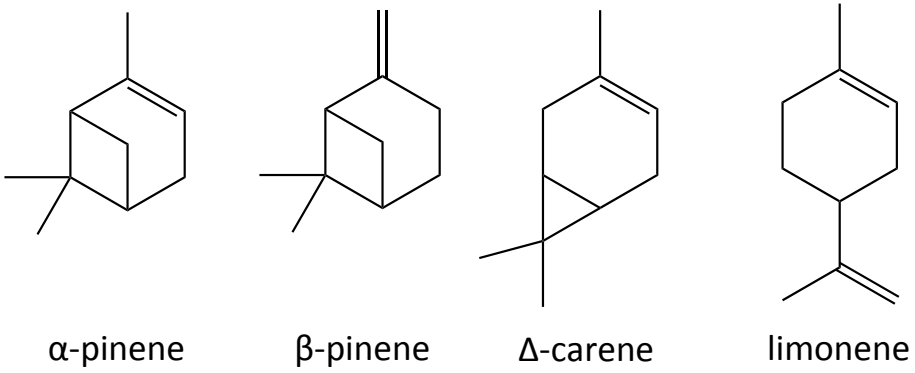

Figure 1. Structures of monoterpenes used in this study.

ACPD
15, 14923–14960, 2015

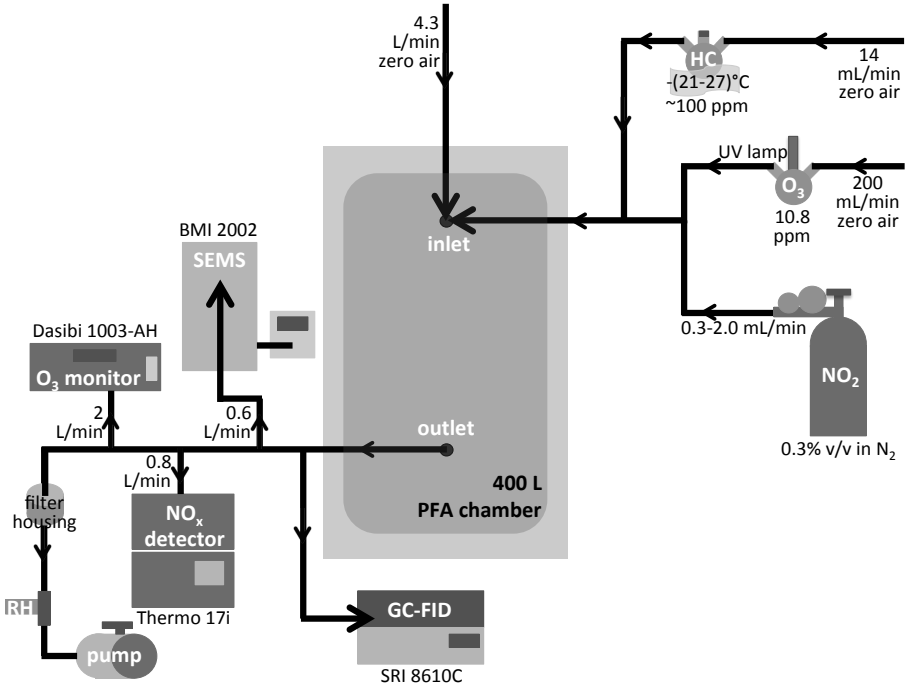

Figure 2. Reed Environmental Chamber (REC) schematic for the experiments described here.

ACPD
15, 14923–14960, 2015

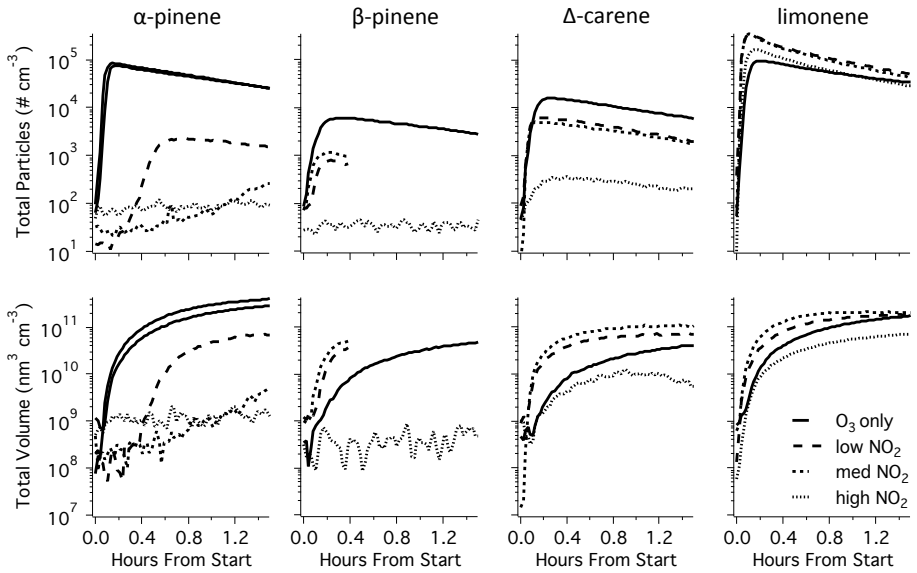

Figure 3. Raw total number concentrations (N_{tot}) and total volume concentrations (V_{tot}) at each NO_2 concentration for each monoterpene studied, not corrected for wall losses.

ACPD
15, 14923–14960, 2015

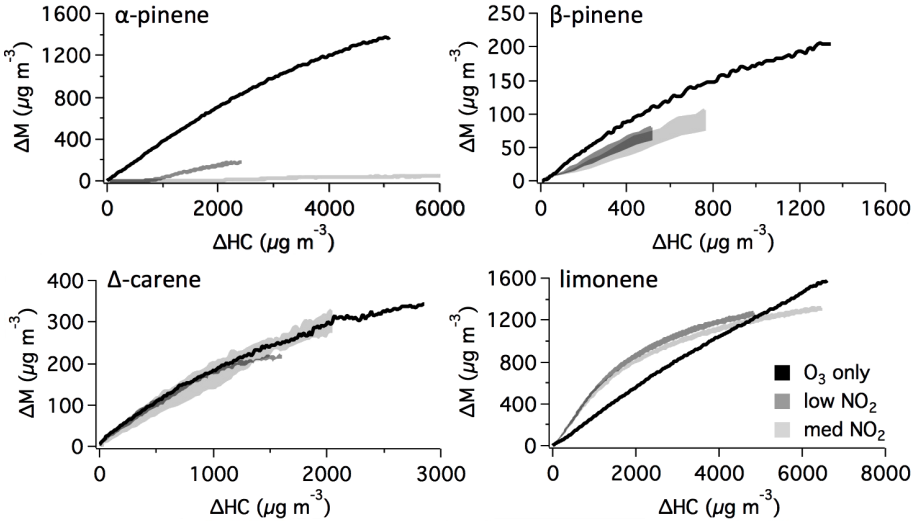

Figure 4. Δ*M* vs. ΔHC for each experiment. Δ*M* is corrected for wall losses (described in Supplement). Uncertainty ranges arise from modeled ΔHC values using the range of 10^{-15} to 10^{-12} cm^3 molec^{-1} s^{-1} for $k_{RO_2+RO_2}$ for the low and medium NO_2 experiments for each monoterpene. O_3-only experiments do not have an analogous uncertainty range since all O_3 was assumed to react with the monoterpene directly.

ACPD
15, 14923–14960, 2015

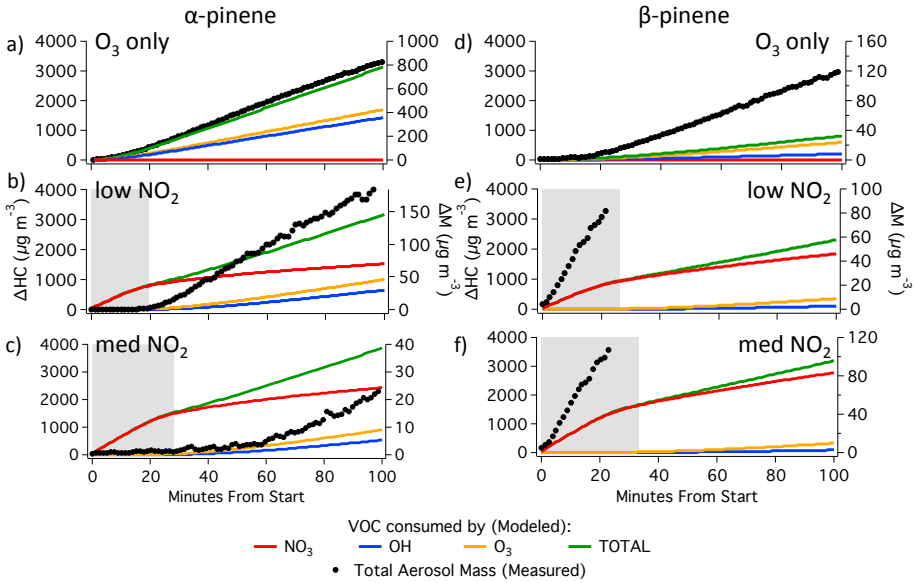

Figure 5. Time series of wall loss corrected aerosol mass (right axis) and VOC consumed by each oxidant (left axis) for α-pinene and β-pinene at zero **(a, d)**, low **(b, e)**, and medium **(c, f)** NO_2 concentrations, highlighting how much aerosol is produced at times dominated by NO_3-oxidation (shaded regions). ΔHC values shown are the lower limits calculated using the lowest $RO_2 + RO_2$ rate constant (10^{-15} cm^3 molec^{-1} s^{-1}), which gives the low limit on how much NO_3 reacts with VOC directly.

ACPD
15, 14923–14960, 2015

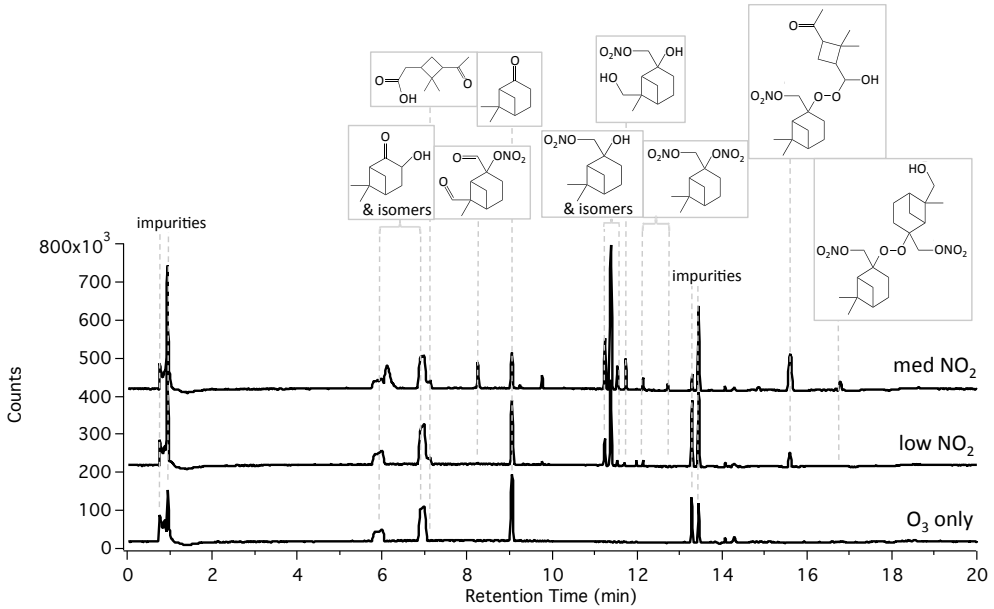

Figure 6. Comparison of chromatograms from HPLC-ESI-MS samples of SOA derived from β-pinene ozonolysis with 0 (bottom), 530 (middle), and 910 ppb NO_2 (top). Chromatograms are annotated with speculative structures corresponding to the most intense peaks. Proposed structures are listed in Table S.3 based on products observed in other studies, but may actually be isomers of the structures shown.

ACPD
15, 14923–14960, 2015

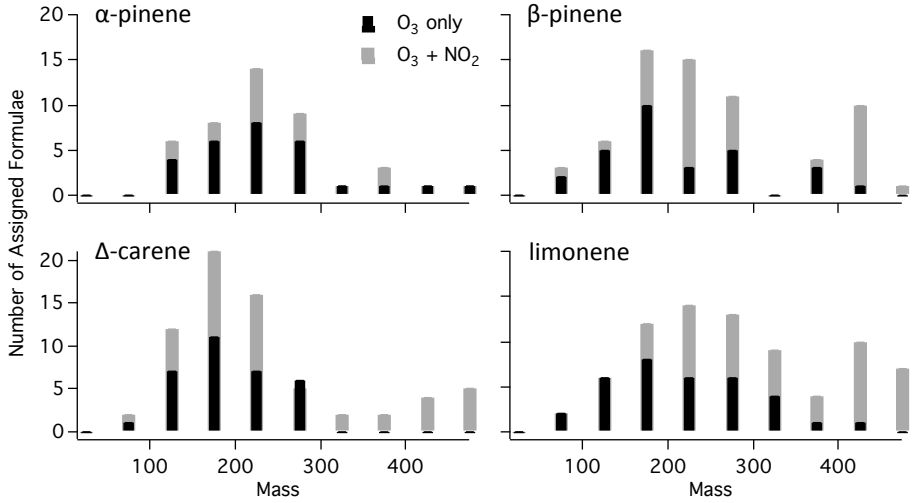

Figure 7. Histograms of each O_3 vs. NO_3 ($O_3 + NO_2$) regime for each monoterpene showing the number of compounds (left axis) in each 50 amu mass bin (bottom axis).

ACPD
15, 14923–14960, 2015